The Transition State for Intramolecular Atom Exchange between Hydride and Dihydrogen Ligands in *cis*-$[Fe(PR_3)_4H(H_2)]^+$ Complexes. Trishydride or Trihydrogen?

Heiko Jacobsen[†]

Universität Zürich, Winterthurerstrasse 190, CH-8057 Zürich, Switzerland

Received: March 7, 2002

The structure and bonding of *cis*-$[Fe(PH_3)_4H(H_2)]^+$, as well as of the transition state for intramolecular hydrogen exchange is investigated by pure density functional calculations (BP86), as well as by hybrid methods (B3LYP). The calculated Fe−P distances as well as the Fe−H separations of the dihydrogen ligand are significantly longer in the B3LYP case than for BP86. Both sets of calculations predict a low activation energy for intramolecular hydrogen exchange, consistent with experimental findings, but the value of $\Delta E^{\ddagger}$ is twice as large for B3LYP compared to that of BP86 (19 and 9 kJ/mol, respectively). The chemical bonding is described according to a topology analysis of the electron density, based on the theory of "atoms in molecules". According to the BP86 calculations, the transition state for the intramolecular hydrogen exchange process clearly has to be classified as a trishydride complex, whereas the B3LYP approach not only results in Fe−H bonds but also in H−H bonding interactions, thus suggesting the presence of a trihydrogen moiety.

Introduction

The concept of stereochemically nonrigid stuctures[1] is one of the important aspects in modern coordination chemistry, and the "neglect of the effect of dynamics on stereochemistry can lead to serious misconceptions and, at the very least, is a step removed from reality".[2] In particular, hydride fluxionality in transition metal complexes[3] has played a key role in developing mechanistic concepts, as can be seen from the pioneering papers of Muetterties and co-workers on complexes of the type $Fe(PR_3)_4H_2$.[4] With the discovery of molecular dihydrogen complexes,[5] a new research topic was added to the field of transition metal hydride chemistry. Protonated complexes of the type $[Fe(PR_3)_4H(H_2)]^+$ with monodentate phosphine ligands became an interesting target, and have been recognized[6] as one of the first examples of transition metal complexes in which a hydride as well as a dihydrogen ligand coexist. The possible interchange of a hydrogen atom then makes these hydride−dihydrogen complexes the simplest model for σ-bond activation reactions.[7]

The first *ab initio* studies on this type of compounds were presented by Maseras and co-workers, who not only investigated several coordination geometries for the model complex $[Fe(PH_3)_4H(H_2)]^+$ **1**[8] but also addressed the intramolecular atom exchange between the hydride and the dihydrogen moiety for the *cis*-geometry of **1**.[9] They conclude that the favored mechanism is the so-called open direct transfer, which consists of a single step transfer of the hydrogen atom between the two ligands. In the transition state of this mechanism, the central hydrogen atom is bound to the metal center and to the other two hydrogens. According to the calculations of Maseras and co-workers, this process is associated with an activation energy of 13 kJ/mol. For the transition state of an addition−elimination reaction, which would involve a true transition metal trihydride, a barrier of 273 kJ/mol was reported.[9]

We have recently presented density functional[10] (DF) calculations on complexes of the type $[M(P(CH_3)_3)_4H(H_2)]^+$ (M = Fe, Ru, and Os),[11] and in this context compared the model complex $[Fe(PH_3)_4H(H_2)]^+$ **1** with the real molecule $[Fe(P(CH_3)_3)_4H(H_2)]^+$.[12] For the *cis*-geometry of the latter compound, our calculations indicate that the transition state for hydrogen exchange might indeed be characterized as a trihydride complex. Here, we want to reexamine this problem, and present DF calculations on the hydrogen exchange process for the *cis*-geometry of **1**. The chemical bonding will be analyzed following concepts developed in the theory of atoms in molecules (AIM),[13] which provide a clear definition of a chemical bond by means of a topology analysis of the electron density $\rho(\mathbf{r})$. We further compare BP86-DF calculations, where gradient corrections for exchange and correlation were taken from the work of Becke[14] and Perdew,[15] respectively, with hybrid-DF[16] calculations with the B3LYP functional.[17] The surprising results of this comparison will be discussed in detail in the next section.

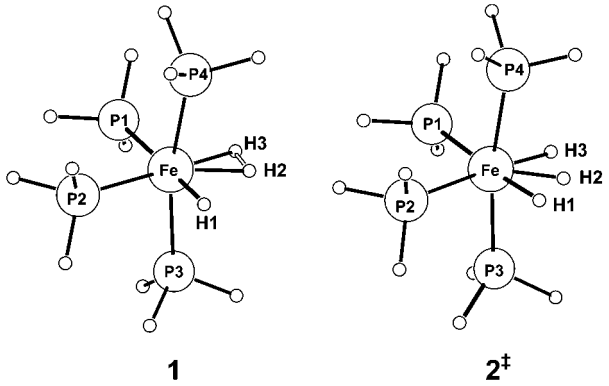

Figure 1. Molecular geometries of $[Fe(H)_3(PH_3)_3]^+$. Ground state **1** and transition state for intramolecular hydrogen exchange $\mathbf{2}^{\ddagger}$.

Results and Discussion

In Figure 1, exemplary geometries for the local minimum of the *cis*-geometry **1** as well as for the transition state for hydrogen exchange $\mathbf{2}^{\ddagger}$ are displayed. The corresponding structural parameters are collected in Table 1. A brief inspection of these data reveals the fact that both DF methods B3LYP and BP86

[†] Present address: KemKom, 1864 Burfield Ave., Ottawa, Ontario, K1J 6T1, Canada.

10.1021/jp0257404 CCC: $22.00
Published on Web 06/04/2002

TABLE 1: Optimized Geometries for $[Fe(PH_3)_4H(H_2)]^+$ Compared with the X-ray Strucure of $[Fe(P(CH_3)_3)_4H(H_2)]^+$ [a]

	B3LYP		BP86		X-ray
	1	**2‡**	**1**	**2‡**	$[Fe(P(CH_3)_3)_4H(H_2)]^+$
d(Fe−H1)	152	154	152	153	153
d(Fe−H2)	161	150	156	148	156
d(Fe−H3)	164	154	159	153	187
d(H1−H2)	178	114	173	125	195
d(H2−H3)	83	114	90	125	94
d(Fe−P1)	230	228	224	223	226
d(Fe−P2)	226	228	221	223	221
d(Fe−P3)	228	229	223	223	223
d(Fe−P4)	228	229	223	223	223
∠(H1−Fe−H2)	69	44	68	49	78
∠(H2−Fe−H3)	30	44	33	49	30
∠(H1−Fe−P2)	81	86	80	82	84
∠(H3−Fe−P1)	82	86	81	82	73
∠(P1−Fe−P2)	97	100	97	98	94
∠(P3−Fe−P4)	165	170	166	168	152

[a] Distances in picometers, angles in degree.

SCHEME 1

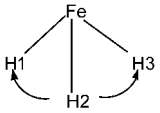

result in similar bond angles, but significantly differ in the bond length for the phosphine and dihydrogen ligands. In particular, the Fe−P bonds are calculated to be longer by 5 to 6 pm using the hybrid functional. In this case, the Fe−H separations for the dihydrogen ligand too are longer by 5 pm. Consequently, the H−H bond elongation, caused by σ-donation as well as σ^*-back-donation,[18] is larger by 7 pm in the BP86 case, indicating a somewhat more thermodynamically activated dihydrogen complex. It should also be noted that in both cases the Fe−H bond distance for the hydride is identical.

We can compare our optimized geometries with the crystal structure of $[Fe(P(CH_3)_3)_4H(H_2)]^+$,[19] for which selected structural parameters are added to Table 1. The significant differences in the bond angles are due to the different donor capabilities of PH_3 and $P(CH_3)_3$ ligands, which we have shown before in calculations on the model system **1** and on the real molecule.[12] Also, in view of the high standard deviations of the hydrogen positions in the X-ray diffraction study, we will not comment on the coordination geometry of the dihydrogen and the hydride ligands. Calculations and experiment are consistent in fact that the P1 ligand in *trans*-position to the hydride forms the longest Fe−P bond, whereas the P2 ligand in *trans*-position to the dihydrogen ligand shows the shortest Fe−P separation. The agreement in the values for Fe−P distances is excellent in case of the BP86 calculation, which seems to be the better computational approach in this particular case.

The transition state **2‡** is characterized by one negative frequency, which amounts to -1068 cm^{-1} and -742 cm^{-1} for the B3LYP and BP86 calculation, respectively. The negative frequency corresponds to the wagging mode of the H2 atom, as shown in Scheme 1, therefore characterizing simultaneous H2−H3 bond breaking and H2−H1 bond making.

The activation energy for this process amounts to 19 kJ/mol for the B3LYP case, but only to 9 kJ/mol for BP86. This result was anticipated, since already the optimized geometries indicated that BP86 calculations predict a more activated dihydrogen ligand. The calculated activation energies correspond well with the experimental fact that very fast H/H_2 scrambling is observed even at temperatures as low as -140 °C.[19]

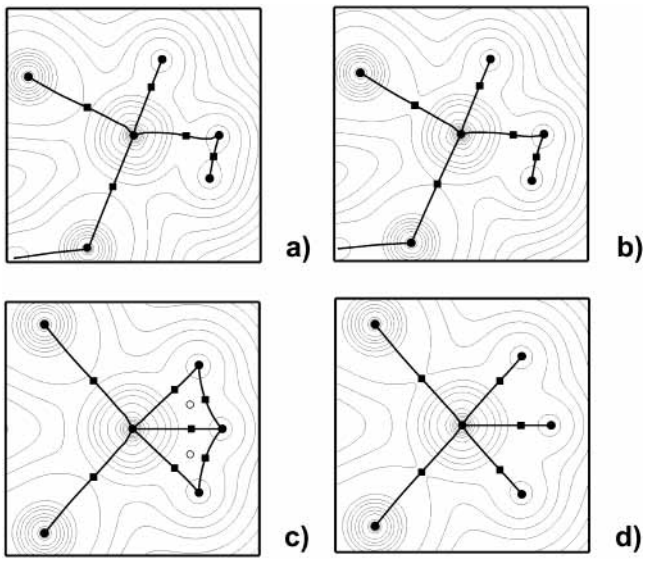

Figure 2. Contour lines of the charge density (thin) and molecular graphs (bold) in the Fe−H1−H2−H3 plane for (a) B3LYP-**1**, (b) BP86−**1**, (c) B3LYP-**2‡**, and (d) BP86-**2‡**. Bond critical points are indicated by filled squares (■), ring critical points by open circles (○).

SCHEME 2

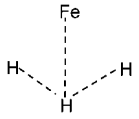

Maseras and co-workers described the transition state for hydrogen exchange **2‡** as a trihydrogen connected to the metal via its central atom, as depicted in Scheme 2.

They also note that no four membered ring exists in the transition state, which would correspond to the traditional view of σ-bond metathesis. If we compare our transition state geometries with the one reported by Maseras and co-workers, we will see substantial differences. In particular, the DF calculations result in H−H separations being 10−20 pm longer, and Fe−H distances being 6−13 pm shorter than found in the early *ab initio* calculations. This again might be a first indication that the DF calculations suggest that the transition state structure should be described as trishydride rather than a trihydrogen complex.

To get a better understanding of the problem, a topological analysis of the electron density $\rho(\mathbf{r})$ was performed, based on the theory of "atoms in molecules" (AIM).[13] This analysis might be used to assess the chemical bonding situation in a given molecule. In particular, gradient paths of the gradient vector field $\nabla\rho(\mathbf{r})$, which originate at a bond critical point and terminate at the nuclei, might be used to define a chemical bond, and to establish a molecular graph.[20] Such graphs in the Fe−H1−H2−H3 plane of **1** and **2‡** are displayed in Figure 2. Again, it should be noted that the chemical bonds, which define the molecular graph, are derived from the electron density of the calculated molecules, and not from optimized molecular geometries. The AIM approach provides a clear and unambiguous definition of a chemical bond, and is applicable, whenever the electron density $\rho(\mathbf{r})$ is known, be it from theory or experiment.

For the *cis*-geometry **1**, both the B3LYP (Figure 2a) and the BP86 (Figure 2b) calculations result qualitatively in the same molecular topology. It is interesting to note that the dihydrogen molecule is bonded only through the one H atom, which is neighboring the hydride ligand. Substantial differences, however, are observed for the transition state geometries **2‡**. The B3LYP

TABLE 2: Selected Bond Ellipticities ϵ for Structures 1 and $2^{\ddagger}$, Obtained from Hybrid DF and Pure DF Calculations

	B3LYP		BP86	
	1	$2^{\ddagger}$	1	$2^{\ddagger}$
Fe−H1	0.065	0.390	0.013	0.119
Fe−H2	0.306	0.278	0.400	0.109
Fe−H3	-	0.390	-	0.119
H1−H2	-	0.622	-	-
H2−H3	0.056	0.622	0.102	-

method (Figure 2c) leads to a molecular graph which both displays Fe−H as well as H−H bonds. Two ring critical points further support the existence of two three-membered H−Fe-H rings, fused by the central Fe−H bond. One might describe this coordination mode as a trihydrogen unit bonded to the transition metal center not only by one Fe−H bond, as suggested by Maseras and co-workers, but by three Fe−H bonds instead. On the other hand, the BP86 method (Figure 2d) clearly shows the molecular graph of a true transition metal trishydride, lacking any H−H bonds. The different molecular topology might be reasoned by the differences in the transition state geometries. The H−H bond length of 114 pm found for B3LYP-$2^{\ddagger}$ still allows for bonding H−H interaction, whereas the H−H separation of 125 pm as calculated for BP86-$2^{\ddagger}$ results in the trishydride molecule. The significant shorter Fe−H distances found in the BP86 calculations support this observation.

Further information about the chemical bonding might be obtained from the bond ellipticities ϵ, which are defined by the two principal curvatures λ_1 and λ_2 of $\rho(\mathbf{r})$ at the bond critical point as $\epsilon = (\lambda_2/\lambda_1) - 1$, with $\lambda_2 < \lambda_1$. Bond ellipticities not only provide a measure for the π character of a bond, but also for its structural stability.[21] This is to be understood in the sense that bonds with ϵ-values close to zero are classified as stable bonds, whereas substantial deviations from zero reflect their structural instability.[22]

Selected ellipticities for Fe−H and H−H bonds of **1** and $2^{\ddagger}$ are collected in Table 2.

The fact that ϵ_{H2-H3} is twice as large for BP86-**1** compared to B3LYP-**1** might again be taken as an indication that the hybrid DF calculation results in a less activated dihydrogen molecule, as we have already concluded before from activation energies and transition state geometries. Comparing ϵ_{Fe-H1} and ϵ_{Fe-H2}, we observe that the bonded dihydrogen molecule is structurally much less stable than the hydride ligand.

Turning to the transition state geometry, the situation for B3LYP-$2^{\ddagger}$ is the most interesting. We see that the values for ϵ_{Fe-H} are roughly twice as large as the ones for ϵ_{H-H}. It is tempting to follow Cioslowski and Mixon and interpret the aforementioned gradient paths as interaction lines delineating major—not necessarily bonding—interactions present within a given chemical system.[23] Given this definition, as well as the values for ϵ_{Fe-H} and ϵ_{H-H}, one might then interpret the H1−H2 and H2−H3 gradient paths (Figure 2c) as "attractor interaction lines between nonbonded atoms".[24] Thus, B3LYP-$2^{\ddagger}$ would also classify as a trishydride complex, supported by additional H−H interactions. However, in a recent careful analysis Bader states that "no repulsive forces act on atoms linked by a bond path, nor on their nuclei".[20] This implies that B3LYP-$2^{\ddagger}$ might indeed be described as a trihydrogen complex, in which the trihydrogen fragments bonds via all three H atoms to the metal center.

Conclusion

In the present work, we have explored structure and bonding of the model complex $[Fe(PH_3)_4H(H_2)]^+$ **1**, using BP86 DF calculations, as well as B3LYP hybrid DF calculations. The results of the two DF approaches significantly differ from each other. Regarding the optimized geometries, the Fe−P distances as well as the Fe−H separations of the dihydrogen ligand are significantly longer in the B3LYP case than for BP86. Comparison with X-ray structures[19] and other DF calculations[12] suggests that the BP86 approach results in a better description of the molecular geometries. Both sets of calculations predict a low activation energy for intramolecular hydrogen exchange, consistent with experimental findings,[19] but the value of $\Delta E^{\ddagger}$ is twice as large for B3LYP compared to that for BP86. Qualitative differences appear in the topological description of the chemical bonding in the transition state $2^{\ddagger}$ for the hydrogen exchange process. According to the BP86 calculations, this structure clearly has to be classified as a trishydride complex, whereas the B3LYP approach not only results in Fe−H bonds but also in H−H bonding interactions. To decide whether the pure or the hybrid DF approach leads to the better electron densities $\rho(\mathbf{r})$, more comparative studies of transition metal complexes exhibiting unusual chemical bonding situations are needed, especially for cases which allow a direct comparison with experiment.[25] The present work exemplifies that different DF approaches do not only result in *quantitatively* different results, but also give *qualitatively* different descriptions.

Computational Details

Density functional calculations were carried out using the Gaussian98 program system.[26] B3LYP calculations[17] utilize Becke's three parameter hybrid functional[16] together with the correlation functional of Lee, Yang, and Parr.[27] For BP86 calculations, gradient corrections were taken from the work of Becke,[14] and the local correlation functional of Perdew[28] together with his correlation gradient corrections[15] was used. H and P atoms where described by a 6-31G(d,p) basis set.[29] For geometry optimizations and frequency calculations, the transition metal center was described by an effective core potential with the corresponding (8s7p6d1f)/[6s5p3d1f] valence basis set.[30] This set was reduced to (8s7p6d)/[6s5p3d] in the topological analysis of the density, which was performed using the program MORPHY.[31]

Acknowledgment. Access to the computing facilities at the Rechenzentrum der Universität Zürich is gratefully acknowledged. The author thanks Dr. G. I. Nikonov for fruitful discussions.

Supporting Information Available: Cartesian coordinates for optimized geometries of all molecules. This material is available free of charge via the Internet at http://pubs.acs.org.

References and Notes

(1) Muetterties, E. L. *Acc. Chem. Res.* **1970**, *3*, 266.
(2) Muetterties, E. L. *Inorg. Chem.* **1965**, *4*, 769.
(3) Gusev, D. G.; Berke, H. *Chem. Ber.* **1996**, *129*, 1143.
(4) (a) Tebbe, F. N.; Meakin, P.; Jesson, J. P.; Muetterties, E. L. *J. Am. Chem. Soc.* **1970**, *92*, 1068. (b) Meakin, P.; Guggenberger, L. J.; Jesson, J. P.; Gerlach, D. H.; Tebbe, F. N.; Peet, W. G.; Muetterties, E. L. *J. Am. Chem. Soc.* **1970**, *92*, 3482. (c) Meakin, P.; Muetterties, E. L.; Tebbe, F. N.; Jesson, J. P. *J. Am. Chem. Soc.* **1971**, *93*, 4701. (d) Meakin, P.; Muetterties, E. L. Jesson, J. P. *J. Am. Chem. Soc.* **1973**, *95*, 75.
(5) (a) Kubas, G. J. *Acc. Chem. Res.* **1988**, *21*, 120. (b) Kubas, G. J. *Comments Inorg. Chem.* **1988**, *7*, 15.
(6) Albertin, G.; Antoniutti, S.; Bordignon, E. *J. Am. Chem. Soc.* **1989**, *111*, 2072.
(7) (a) Crabtree, R. H. *Chem. Rev.* **1995**, *95*, 987. (b) Crabtree, R. H. *Chem. Rev.* **1985**, *85*, 245.
(8) Maseras, F.; Duran, M.; Lledós, A.; Bertrán, J. *J. Am. Chem. Soc.* **1991**, *113*, 2879.

(9) Maseras, F.; Duran, M.; Lledós, A.; Bertrán, J. *J. Am. Chem. Soc.* **1992**, *114*, 2922.

(10) (a) Ziegler, T. *Chem. Rev.* **1991**, *91*, 651. (b) Kohn, W.; Becke, A. D.; Parr, R. G. *J. Phys. Chem.* **1996**, *100*, 12974. (c) Baerends, E. J.; Gritsenko, O. V. *J. Phys. Chem. A* **1997**, *101*, 5383. (d) Koch, W.; Holthausen, M. C. *A Chemist's Guide to Density Functional Theory*, Wiley-VCH: Weinheim, 2000.

(11) Jacobsen, H.; Berke, H. *Chem. Ber./Rec.* **1997**, *130*, 1273.

(12) Jacobsen, H.; Berke, H. *Chem. Eur. J.* **1997**, *3*, 881.

(13) (a) Bader, R. F. W. *Acc. Chem. Res.* **1985**, *18*, 9. (b) Bader, R. F. W. *Chem. Rev.* **1991**, *91*, 893. (c) Bader, R. F. W.; Popelier, P. L. A.; Keith, T. A. *Angew. Chem., Int. Ed. Engl.* **1994**, *33*, 620. (d) Bader, R. F. W. *Atoms in Molecules. A Quantum Theory*; Clarendon Press: Oxford, 1990. (e) Popelier, P. L. A. *Atoms in Molecules. An Introduction*; Pearson Education: Harlow, 1999.

(14) Becke, A. D. *Phys. Rev. A* **1988**, *38*, 3098.

(15) Perdew, J. P. *Phys. Rev. B* **1986**, *33*, 8822.

(16) (a) Becke, A. D. *J. Chem. Phys.* **1993**, *98*, 1372. (b) Becke, A. D. *J. Chem. Phys.* **1993**, *98*, 5648.

(17) Stephens, P. J.; Devlin, F. J.; Chabalowski, C. F.; Frisch, M. J. *J. Phys. Chem.* **1994**, *98*.

(18) Li, J.; Dickson, R. M.; Ziegler, T. *J. Am. Chem. Soc.* **1995**, *117*, 11482.

(19) Gusev, D. G.; Hübener, R.; Burger, P.; Orama, O.; Berke, H. *J. Am. Chem. Soc.* **1997**, *119*, 3716.

(20) Bader, R. F. W. *J. Phys. Chem. A* **1998**, *102*, 7314.

(21) Popelier, P. L. A.; Logothetis, G. *J. Organomet. Chem.* **1998**, *555*, 101.

(22) Cremer, D.; Kraka, E.; Slee, T. S.; Bader, R. F. W.; Lau, C. D. H.; Nguyen-Dang, T. T.; MacDougall, P. J. *J. Am. Chem. Soc.* **1983**, *105*, 5069.

(23) Cioslowski, J.; Mixon, S. T. *Can. J. Chem.* **1992**, *70*, 443.

(24) Cioslowski, J.; Edgington, L.; Stefanov, B. B. *J. Am. Chem. Soc.* **1995**, *117*, 10381.

(25) Scherer, W.; Hieringer, W.; Spiegler, M.; Sirsch, P.; McGrady, S.; Downs, A. J.; Haaland, A.; Pedersen, B. *Chem. Commun.* **1998**, 2471.

(26) Frisch, M. J.; Trucks, G. W.; Schlegel, H. B.; Scuseria, G. E.; Robb, M. A.; Cheeseman, J. R.; Zakrzewski, V. G.; Montgomery, J. A., Jr.; Stratmann, R. E.; Burant, J. C.; Dapprich, S.; Millam, J. M.; Daniels, A. D.; Kudin, K. N.; Strain, M. C.; Farkas, O.; Tomasi, J.; Barone, V.; Cossi, M.; Cammi, R.; Mennucci, B.; Pomelli, C.; Adamo, C.; Clifford, S.; Ochterski, J.; Petersson, G. A.; Ayala, P. Y.; Cui, Q.; Morokuma, K.; Malick, D. K.; Rabuck, A. D.; Raghavachari, K.; Foresman, J. B.; Cioslowski, J.; Ortiz, J. V.; Stefanov, B. B.; Liu, G.; Liashenko, A.; Piskorz, P.; Komaromi, I.; Gomperts, R.; Martin, R. L.; Fox, D. J.; Keith, T.; Al-Laham, M. A.; Peng, C. Y.; Nanayakkara, A.; Gonzalez, C.; Challacombe, M.; Gill, P. M. W.; Johnson, B. G.; Chen, W.; Wong, M. W.; Andres, J. L.; Head-Gordon, M.; Replogle, E. S.; Pople, J. A. *Gaussian 98*, revision A.5; Gaussian, Inc.: Pittsburgh, PA, 1998.

(27) Lee, C.; Yang, W.; Parr, R. G. *Phys. Rev. B* **1988**, *37*, 785.

(28) Perdew, J. P.; Zunger, A. *Phys. Rev. B* **1981**, *23*, 5048.

(29) (a) Hehre, W. J.; Ditchfield, R.; Pople, J. A. *J. Chem. Phys.* **1971**, *54*, 724. (b) Hehre, W. J.; Ditchfield, R.; Pople, J. A. *J. Chem. Phys.* **1972**, *56*, 2257. (c) Hariharan, P. C.; Pople, J. A. *Theor. Chim. Acta* **1973**, *28*, 213.

(30) Dolg, M.; Wedig, U.; Stoll, H.; Preuss, H. *J. Chem. Phys.* **1987**, *86*, 866.

(31) Popelier, P. L. A. *Comput. Phys. Commun.* **1996**, *92*, 212.